36th International Electric Vehicle Symposium and Exhibition (EVS36)
Sacramento, California, June 11-14, 2023

Size matters: Multi-use Optimization of a Depot for Battery Electric Heavy-Duty Trucks

Florian Biedenbach[1], Yannic Blume[1]
[1]*Forschungsstelle für Energiewirtschaft e.V., Am Blütenanger 71, 80995 Munich, fbiedenbach@ffe.de*

Executive Summary

Battery electric trucks offer a high battery capacity and good plannability, making them attractive for the implementation of bidirectional charging strategies. Nevertheless, most of the previous charging strategy studies focus on electric passenger cars. These charging strategies are usually formulated as separate use-cases like *Tariff-Optimized Charging*, *Arbitrage Trading*, *Peak-Shaving* and *Self-Consumption Optimization*. By using a linear optimization model, we examine these use-cases based on real data from an exemplary depot for battery electric trucks. We combine the use-cases within a multi-use optimization. The optimization results in annual savings of 2,200 EUR per truck for a base scenario with a self-consumption rate of 95%. A sensitivity analysis shows that significantly higher revenues of up to 11,000 EUR per vehicle are possible. Overall, this paper clarifies that depots for electric trucks can offer enormous flexibility and that freight forwarders can benefit strongly from bidirectional charging.

Keywords: heavy-duty, V2G (vehicle to grid), V2V (vehicle to vehicle), simulation, photovoltaic

1 Introduction

Controlled and bidirectional charging has recently become a extensively discussed topic. A variety of publications that deal with this technology predict its high relevance in the near future [1, 2]. The Original Equipment Manufacturers (OEMs) have discovered its importance as well and the first bidirectional vehicles are on the market [3]. Nevertheless, past considerations have mostly revolved around battery electric vehicle (BEV) passenger cars and not focused on battery electric heavy-duty trucks (BET). However, taking into account that heavy-duty and bus traffic is responsible for 6% of all European greenhouse gas emissions, a major wave of electrification in this area is necessary [4]. BET have a number of advantages over passenger cars, which make them highly suitable for controlled and bidirectional charging. Due to the higher charging power and the bundling of many vehicles in one depot, a high marketable capacity can be achieved quickly at one location making less small-scale aggregation necessary.
Previous work on BET is often a comparison of the technology with diesel or hydrogen-based power trains in terms of CO2 emissions, costs, and technical feasibility [5, 6, 7]. Those studies usually predict BETs significantly better emissions and costs in the future, but the availability of BETs with sufficient battery capacity for long-haul transport is noted as an issue [8, 6]. Apart from a few [7], most of these studies are assumption-based and use synthetic driving profiles. When it comes to the optimization of charging processes for BET, there are significantly fewer studies. A study that already examines the optimization of charging processes for BET is [9]. In this paper, the route of the BET is optimized but variable prices are not considered. A similar approach to the method presented in this paper is developed in [10], where the authors optimize the charging processes for trucks in a depot based on the charging costs and also include bidirectional charging. However, the produced results are based on very strong assumptions since assumed driving profiles and a simplified price structure is used. Furthermore, the examination of single days makes the results not reliable.

Even though most of previous work on the topic of charging management and optimization of charging strategies excludes BETs, there is a large amount of literature focusing on passenger cars. Depending on their objective, existing studies distinguish between different use-cases of controlled and bidirectional charging. These use-cases have mostly been considered separately in previous studies [11]. For the use-case *Self-Consumption Optimization*, the self-consumption rate is maximized by shifting charging processes in times with PV generation[2, 12]. Minimizing the peak load at a grid connection point is objective of the use-case *Peak-Shaving* [13]. The optimization of charging with a variable electricity tariff, where charging processes are shifted in times with low prices, can be referred to as *Tariff-Optimized Charging* [14]. The vehicles charge at times when electricity prices are low, and feed the electricity back into the grid at times when electricity prices are high, in the use-case *Arbitrage Trading* [15]. To increase the economic efficiency, use-cases can also be combined in a so-called multi-use-objective, witch has already been investigated for stationary storage facilities [16, 17]. Apart from [11], this methodology has not yet been applied to BEVs and especially not to BETs.
Therefore, we see a need for further research in optimizing charging processes for BETs, especially with regard to multi-use optimization. In this paper, we will tackle this research gap by developing a model to combine the use-cases Self-Consumption Optimization, Peak-Shaving, Tariff-Optimized-Charging and Arbitrage-Trading within a multi-use optimization. This model is applied to a real depot for BETs. The developed model and input data is described in Chapter 2. By using the model, possible savings from bidirectional charging of the BET are determined and presented and discussed in Chapter 3. The final conclusion and an outlook can be found in Chapter 4. The results of this study can be used by freight forwarders and OEMs as an orientation for expectable savings and for the prioritization of charging strategies.

2 Method

2.1 Optimization Model

The optimization model *eFlame* was primarily developed to optimize several use-cases for bidirectional charging separately. In [15, 18], the use-cases Arbitrage-Trading and Self-Consumption Optimization are published. The use-case Peak-Shaving is published in [13]. New in this paper is the combination of the use-cases in the context of a multi-use optimization that was not implemented before. Figure 1 shows all power flows relevant for the optimization. At this point, we describe the optimization problem, covering decision variables, objective function, and constraints. Since the model was primarily developed for optimizing battery electric cars, the vehicles are generally referred to as EVs in the following model description.

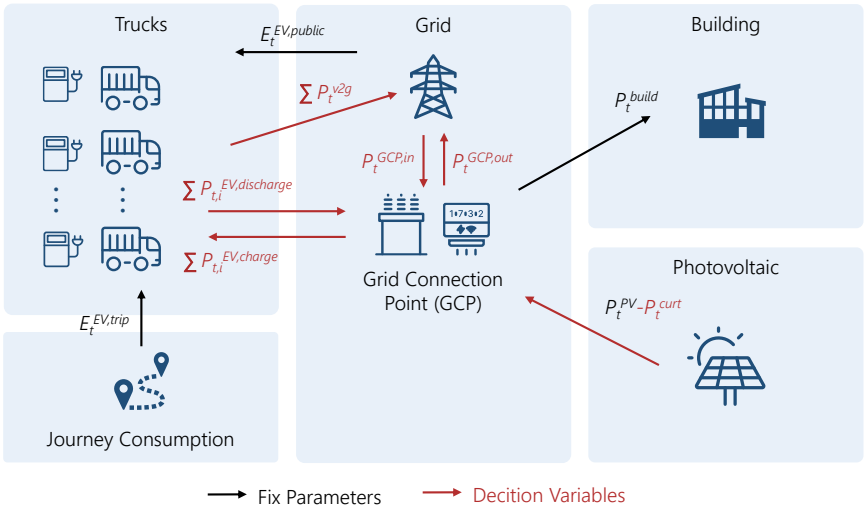

Figure 1: Schematic representation of the optimization model.

For all decision variables the non-negativity constraint applies. The constraint is exemplarily defined in Equation (1) for the received power $P_t^{GCP,in}$ and the fed-in power $P_t^{GCP,out}$ at the Grid Connection Point (GCP), but can be applied to the remaining decision variables. The total number of time steps t in the observation horizon is represented by n.

$$P_t^{GCP,in} \geqslant 0, \qquad P_t^{GCP,out} \geqslant 0 \qquad \forall\, t \in T = \{1, ..., n\} \tag{1}$$

The Photovoltaic (PV) generation is not a decision variable, but it can be influenced during the optimization via the curtailment P_t^{curt}. With this optimization variable, the generation of the PV system can be reduced, e.g. to prevent feed-in at negative prices. Using the decision variable $P_t^{GCP,peak}$, the maximum power at the grid connection point is determined. The charging power P_t^{charge} and discharging power $P_t^{discharge}$ and the energy capacity of the battery E_t^{EV} are further decision variables that are related to the EVs. Furthermore, there is the decision variable P_t^{v2g}, which is used to observe how much energy from the vehicles is fed back into the grid. The remaining decision variables b_t^{charge}, $b_t^{discharge}$, b_t^{out} and b_t^{in} are boolean variables, which are used to ensure that the power of the vehicles and the grid connection point always flows in only one direction.
The objective of the optimization model is to maximize the revenue. The established objective function shown in Equation (2) consists of four terms: the cashflow from arbitrage trading at the spotmarket CF^{spot}, costs through levies C^{levies}, costs through grid fees $C^{gridfee}$, and a term that evaluates the opportunity costs due to battery degradation $C^{bat,deg}$. The different terms are defined in the following.

$$max\left(CF^{spot} + C^{levies} + C^{gridfee} + C^{bat,deg}\right) \tag{2}$$

The cash flow, the difference between cash in- and outflows, from arbitrage-trading at the spot market CF^{spot} is calculated in Equation (3). Different market data can be selected for the price time series p_t^{in} and p_t^{out}, but constant values also can be used.

$$CF^{spot} = \sum_{t=1}^{n} \left(P_t{}^{GCP,in} \cdot p_t^{in} \cdot \Delta t - P_t{}^{GCP,out} \cdot p_t^{out} \cdot \Delta t\right) \qquad \forall\, t \in T \tag{3}$$

Consumers have to pay a gridfee $C^{gridfee}$ to the Distibution System Operator (DSO) for the use of the grid infrastructure. In Germany, the gridfee for commercial customers is divided into a usage price p^{usage} and a capacity price p^{cap}. The usage price depends on the energy consumed, whereas the power price depends on the annual peak power. The gridfee is included in the objective function of Equation (4).

$$C^{gridfee} = \sum_{t=1}^{n} P_t{}^{GCP,in} \cdot p^{usage} \cdot \Delta t + P_{t=n}^{GCP,peak} \cdot p^{cap} \qquad \forall\, t \in T \tag{4}$$

Additionally, various taxes and levies are charged on electricity, which are summarized in C^{levies} and shown in Equation (5). Stationary battery storage may be exempt from levies and such an exemption is also being discussed for bidirectional vehicles. The problem is to determine how much energy is actually fed back into the grid. This is especially problematic in combination with PV systems. Via the decision variable P_t^{v2g}, which is used to determine the power fed from the EVs back into the grid, a partially refund of the levies for fed-back electricity is implemented.

$$C^{levies} = \sum_{t=1}^{n} P_t{}^{GCP,in} \cdot p^{levies} \cdot \Delta t - \sum_{t=1}^{n} P_t{}^{v2g} \cdot \left(p^{levies} - p^{levies,v2g}\right) \cdot \Delta t \qquad \forall\, t \in T \tag{5}$$

The calculation of the degradation costs $C_{bat,deg}$ is based on the use of the battery and determined by the decrease of the available capacity C^{loss} from a cycling aging model from [19]. The costs result primarily from the total charge quantity throughput, which is defined by the charging and discharging power. Based on [20], the price of the battery $c_{bat,buy}$ is set to 139 EUR/kWh. $E^{EV,max}$ is the capacity of the battery. The end of life of the battery is set at a loss of 20% of the initial capacity based on [21].

$$C_{bat,deg} = \frac{c_{bat,buy} \cdot E^{EV,max}}{20\%} C_{loss}(P_t^{EV,charge}, P_t^{EV,discharge}) \qquad \forall\, t \in T \tag{6}$$

The optimization model is restricted by several constraints concerning the GCP and the EVs. We start by introducting the boundrary conditions of the GCP. According to the law of conservation of energy, the in-coming power flows at the GCP must be equal to the out-coming power flows. This is ensured by Equation (7). The load profile of the building P_t^{build} is integrated into the optimization as an static time series.

$$P_t^{GCP,in} + \sum_{i=1}^{n_{EV}} P_t^{EV,discharge} + P_t^{PV} = P_t^{GCP,out} + \sum_{i=1}^{n_{EV}} P_t^{EV,charge} + P_t^{curt} + P_t^{build} \qquad \forall\, t \in T \tag{7}$$

For the determination of the gridfee $C^{gridfee}$ in Equation (4), the annual peak power at the GCP $P_t^{GCP,max}$ is required. Using Equation (8), the power peak is updated continuously during the optimization. Thus, the last time step n contains the annual power peak.

$$P_t^{GCP,peak} \geqslant P_t^{GCP,in}, \qquad P_t^{GCP,peak} \geqslant P_{t-1}^{GCP,peak} \qquad \forall\, t \in T \tag{8}$$

Equations (9) and (10) are introduced to prevent energy from being purchased and fed in simultaneously at the GCP. In consequence, the boolean decision variables b_t^{in} and b_t^{out} are used. $P^{GCP,max}$ describes the maximum grid connection capacity, which results from the transformer and structural conditions at the grid connection point. The grid connection capacity is always greater than or equal to the annual power peak.

$$P^{GCP,max} \cdot b_t^{in} \geqslant P_t^{GCP,in}, \qquad P^{GCP,max} \cdot b_t^{out} \geqslant P_t^{GCP,out} \qquad \forall\, t \in T \tag{9}$$

$$b_t^{out} + b_t^{in} \leqslant 1 \qquad \forall t \in T \tag{10}$$

The following constraints are related to the EVs and apply separately for each EV. The energy balance of the vehicle battery must be maintained to preserve the physical consistency of the EVs. The energy stored in the EV battery in the first time step is defined by the constraint Equation (11). For the first time step, this equation defines the stored energy as equal to the initial stored energy plus the charged energy at the GCP and public minus the discharged energy and the energy consumed during trips $E_t^{EV,trip}$. Constant losses for charging $\eta^{EV,charge}$ and discharging $\eta^{EV,discharge}$ are considered.

$$E_{t=1}^{EV} = SOC_{t=1}^{EV} \cdot E^{EV,max} + P_{t=1}^{EV,charge} \cdot \eta^{EV,charge} \cdot \Delta t - P_{t=1}^{EV,discharge} \cdot \eta^{EV,discharge} \cdot \Delta t - E_{t=1}^{EV,trip} + E_{t=1}^{EV,public} \tag{11}$$

For the remaining time steps, Equation (12) applies, where the initial stored energy is replaced by stored energy of the previous time step.

$$E_t^{EV} = E_{t-1}^{EV} + P_t^{EV,charge} \cdot \eta^{EV,charge} \cdot \Delta t - P_t^{EV,discharge} \cdot \eta^{EV,discharge} \cdot \Delta t - E_t^{EV,trip} + E_t^{EV,public} \qquad \forall\, t \in \{2, ..., n\} \tag{12}$$

Equation (13) ensures that the vehicles are always charged with a minimum State of Charge $SOC^{EV,dep,min}$ at departure. The condition is only valid for the time steps in which a vehicle departs, which is implemented with the boolean variable $b_t^{EV,dep}$. This variable is determined before the optimization based on the driving profiles and is only equal to one if the vehicle departs. To ensure that the condition can also be met if the vehicle is only plugged in for a short time and thus the minimum SOC cannot be reached, a buffer E_t^{buffer} is integrated into the condition. This buffer is also determined before the optimization.

$$E_t^{EV} + E_t^{buffer} = SOC^{EV,dep,min} \cdot E^{EV,max} \cdot b_t^{EV,dep} \qquad \forall\, t \in T \tag{13}$$

Apart from public charging, each EV can only be charged or discharged if it is connected to a charging point at the GCP which is ensured by Equation (14) and (15). Therefore, the boolean variable b_t^{EV} is used which is determined before the optimization based on the driving profiles. The variable is always zero, unless the vehicle is plugged-in at the GCP, in which case it is one. We assume that each vehicle has its own charging point. To prevent the EVs from charging and discharging at the same time, the decision variables b_t^{charge} and $b_t^{discharge}$ are added to Equations (14) and (15). Equation (16) prevents both variables from being equal to one simultaneously.

$$b_t^{EV} \cdot b_t^{charge} \cdot P^{EV,charge,max} \geqslant P_t^{EV,charge} \qquad \forall\, t \in T \tag{14}$$

$$b_t^{EV} \cdot b_t^{discharge} \cdot P^{EV,discharge,max} \geqslant P_t^{EV,discharge} \qquad \forall\, t \in T \tag{15}$$

$$b_t^{charge} + b_t^{dischare} \leqslant 1 \qquad \forall\, t \in T \tag{16}$$

Finally, boundary conditions are required to determine the power fed back from the EVs into the grid P_t^{v2g}. This power is necessary to calculate the exemption from levies in Equation (5). Therefore, we choose a power balance based approach and rearrange Equation (7) according to the discharged energy. Since power can only be fed into the grid if no energy is purchased, P_t^{in} is set to zero. The discharged energy is replaced by the introduced decision variable P_t^{v2g}, resulting in Equation (17). The boundary condition in Equation (18) ensures that P_t^{v2g} cannot become greater than the fed-in power. The power P_t^{v2g} is only an auxiliary variable calculated from the other power variables and is therefore not directly included in the power balance.

$$P_t^{v2g} \leqslant P_t^{GCP,out} - P_t^{PV} + P_t^{curt} + P_t^{build} + \sum_{i=1}^{n_{EV}} P_t^{EV,charge} \qquad \forall\, t \in T \tag{17}$$

$$P_t^{v2g} \leqslant P_t^{GCP,out} \qquad \forall\, t \in T \tag{18}$$

Since the model is intended to examine entire years and the use of boolean variables makes it a mixed-integer optimization problem, the computational effort required to solve the problem is very high. In order to be able to solve it with a reasonable computational effort, the model is computed as a rolling optimization. The determination of the annual power peak is a special aspect of the rolling optimization, which will be explained in the following using the schematic diagram in Figure 2. For rolling optimization, the whole optimization period is divided into m smaller optimization time periods with uniform size. In individual optimization steps, each of the smaller optimization periods is optimized one after the other. The results of an optimization step are passed as start values to the next step. By using an overlapping period, we increase the prediction horizon for the optimization. After the m-th step, the first run of the optimization is finished. According to Equation (8), the power peak is continuously updated as shown in Figure 2 below. As can be seen in the figure, the first optimization steps are limited with a lower power peak than the later steps. Therefore, in a second optimization run, the affected steps before the occurrence of the annual power peak are optimized again with the updated power peak.
In the used model *eFlame*, charging is first simulated without optimization as reference (*ref*). Afterwards, the optimization is performed with unidirectional vehicles (*uni*) and finally with bidirectional vehicles (*bidi*).

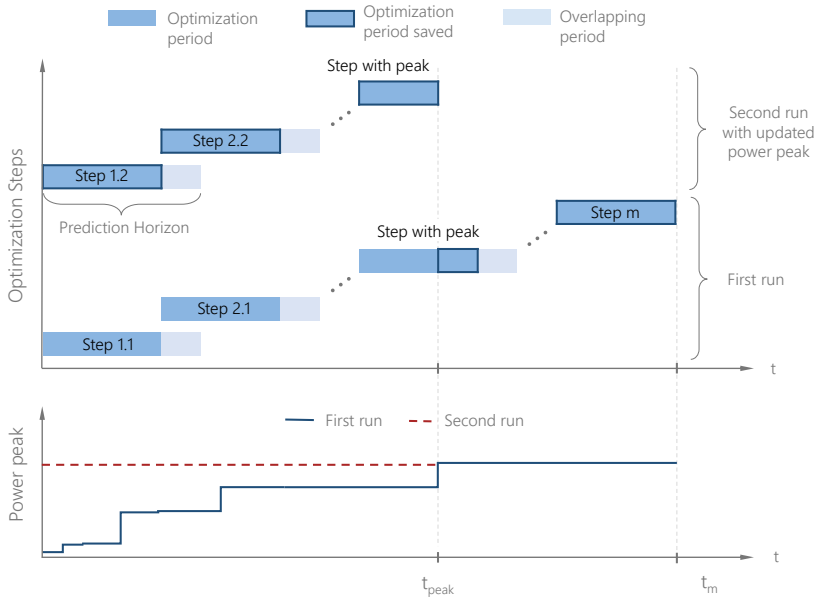

Figure 2: Schematic diagram explaining the used rolling optimization process.

2.2 Input Data

As mentioned in Chapter 1, lots of existing research on the topic of BET is built on assumptions. In this paper, we had the opportunity to use real-life data from a depot of a freight forwarding company from

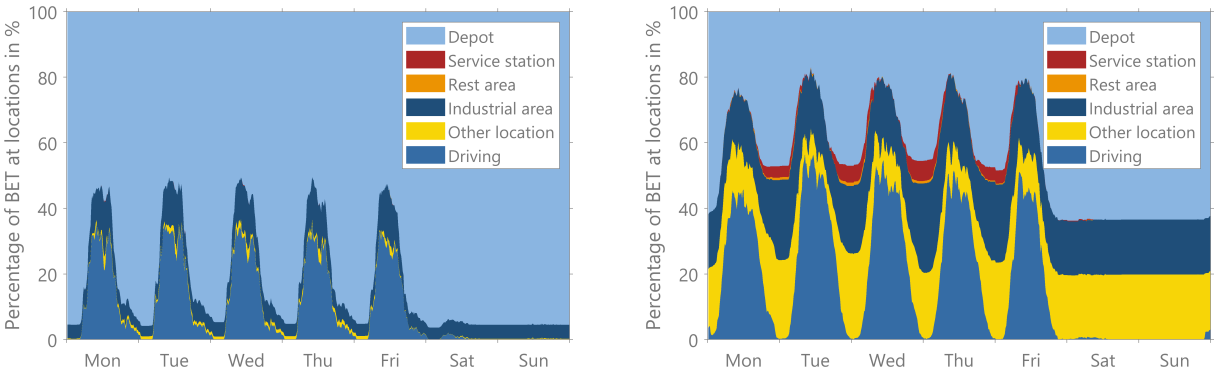

(a) Cluster: Local Transport

(b) Cluster: Distribution Transport

Figure 3: Layered percentage of BET at different locations over the week.

Germany. The company operates mostly local and distribution transport. The data was provided within the framework of the project NEFTON in which partners from industry and science jointly develop a Megawatt Charging System (MCS) for BET. Mobility data of the company's trucks, historical load profiles of their buildings and information about their PV-system are included in the data. The selected depot can not be considered as a representative but as an real-life example.
In the project NEFTON, driving data from several fleets of German fleet operators were recorded using high-resolution GPS data loggers. The recorded data set includes 1.26 million km of driving data and is openly available in anonymized form in [22]. Only the driving data of the depot under consideration was extracted from this data set. Since the data were recorded for diesel trucks, our investigation builds on the simplification that the driving behavior of diesel trucks is transferable to electric trucks. The data is available for different lengths of time and was extended to uniform periods using a Markov process. To avoid oversizing the vehicle batteries, the missions in the dataset are divided into two clusters depending on the distance traveled. Missions with a distance of more than 200 km are grouped into the cluster *Distribution Transport* and those with less than 200 km into the cluster *Local Transport*. Since the process of processing and converting the driving data into annual driving profiles is beyond the scope of this paper, it will be published separately. The annual driving profiles are therefore taken as given and due to their importance for the results of the optimization presented in the following. Figure 3 shows the average percentage of vehicles in different locations for the two clusters. It can be seen that especially the mobility profiles from the Local Transport cluster have very high idle times in the depot and that at least 50% of the BET are always present in the depot. On weekends and at night, most of the vehicles are located in the depot. The driving profiles of the cluster Dirstibution Transport show significantly lower idle times in the depot. During the day on weekdays, 80% of the vehicles are absent. On weekends, almost 40% are not in the depot. In addition, the driving profiles of Distribution Transport show high parking durations in industrial areas and other locations. The difference between the two clusters is also evident from the characteristic values included in Table 1. The annual kilometrage of the Local Transport cluster is approx. 14,000 km, which is significantly lower than the kilometrage of the Distribution Transport cluster of approx. 66,000 km. The electrical consumption for the driving profiles is determined using the model from [23]. The average annual consumption determined in this way is also included in Table 1. The variables $b_t^{EV,dep}$, E_t^{buffer} m b_t^{EV}, $E_t^{EV,trip}$ and $E_t^{EV,public}$ are determined based on the driving profiles and serves as input for the optimization model.

Table 1: Characteristics of the used driving profiles.

Characteristics	Local Transport	Distribution Transport
Daily kilometrage (Weekdays/Weekends)	53,8 km / 0,75 km	250 km / 4,2 km
Percentage at depot (Weekdays/Weekends)	78,20% / 95,19%	37,80% / 63,40%
Annual kilometrage	14.382 km	65.750 km
Average Consumption per km	1,1 kWh/km	1,26 kWh/km
Annual energy consumption	14,9 MWh	83,4 MWh

Besides the driving profiles, the load profile of the building of the depot P_t^{build} is another important input for the optimization. Here, we had once again the opportunity to use real data from the depot. The used load profile is shown in Figure 4a for an average week. From the annual time series, the average was determined for each quarter-hour of the week, as well as the ranges in which 80% and 100% of the

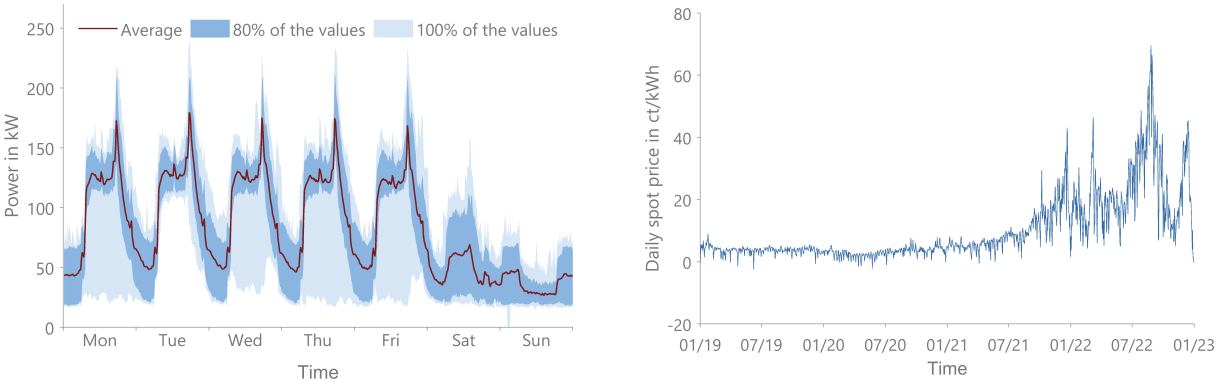

(a) Electric load profile of the depot building

(b) Daily average price intraday auction

Figure 4: Layered percentage of BET at different locations over the week.

values lie. The plot shows that there are significant load peaks in the evening hours on weekdays which indicates that it is suitable for peak shaving. The load is significantly lower at weekends and at night than during the day on weekdays.
We assume that the depot pays variable electricity prices based on the prices of the electricity exchange. Therefore, we used the intraday auction price as electricity price p_t^{in} and p_t^{out} for the optimization. In Europe, there are various short-term markets on the power exchange. One of these markets is the intraday auction. Due to the shorter time slices of quarter hours compared to the day-ahead market, where hourly products are traded, this market offers higher price spreads which increase the revenue opportunities for flexibilities like bidirectional EVs. The development of the prices of the intraday auction from the beginning of 2019 to the end of 2022 is shown in Figure 4b. In consequence of the energy crisis, the price has risen from around 4 ct/kWh to a maximum of over 70 ct/kWh and also the price spreads increased significantly.
The PV generation is determined as a time series depending on the historical irradiation data on CAMS level as a function of the orientation of the PV plant and its peak power [24]. The irradiation data are used for the location of the depot for the weather year 2012.

2.3 Input parameters

After introducing the data source and the model in the previous sections, the input parameters are presented in the following. Therefore, we define a base scenario for which the input parameters are listed in Table 2. By varying different parameters of this base scenario, various sensitivities are examined. For the sensitivity analysis, one parameter of the base scenario is changed respectively while the rest of the parameters are left unchanged. The varied parameters of the sensitivity analysis are also included in the table. The base year is 2021 and the optimization is performed with a time step size of 15 minutes. An observation period of 7 days is used, which consists of the optimization period of 6 days and one day overlap. In the base scenario, no exemption of levies on energy fed back into the grid is assumed, which is why p^{levies} is set to be equal to $p^{levies,v2g}$. However, the exemption is considered in the sensitivity analysis. In the base scenario, no limitation of the grid connection capacity is considered, which is why $P^{GCP,max}$ is set to the oversized value of 5 MW. A limitation of $P^{GCP,max}$ is examined in the sensitivity analysis. The grid connection capacity is minimally limited to 700 kW, since a lower capacity would result in the curtailment of the PV system in times with high irradiation. The feed-in tariff of 0.06 EUR/kWh is an assumed value suitable for Germany which is only used in the reference simulation as p_t^{out}. It is also assumed that 30 BET of the depot, which primarily uses diesel trucks so far, will be electrified. The number of electric vehicles is one of the sensitivities examined. According to the distribution from the data set, 30% of the vehicles are used for distribution traffic and 70% for local traffic. The appropriate driving profiles are divided among the BET according to the distribution and a battery capacity of 250 kWh for local and 500 kWh for distribution traffic is assumed. The parameters for the PV system are selected according to the system of the real depot.
In addition to the year 2021 of the base scenario, the years 2019, 2020, and 2022 are also examined. For the optimization of the different years, several parameters have to be varied, in contrast to the other sensitivity analyses. In consequence, these year-dependent parameters are separated in Table 3. For the reference simulation, a constant price based on the average dayahead price is assumed for p_t^{in} [25]. For the levies, the real historical values for Germany from [26] are used. The prices for the grid fees are also based on historical values of the grid operator Netze BW, where the depot under consideration is located [27]. We use the prices for medium voltage and an annual usage time of less than 2500 h.

Table 2: Parameters of the base scenario and sensitivities.

Category	Parameter	Symbol	unit	Value	Sensitivities
General	year			2021	2019, 2020, 2022
	Size time step	t	h	0.25	
	Optimization period		h	168	
	Overlapping period		h	24	
GCP	Levies on V2G	$p^{levies,v2g}$	EUR/kWh	p^{levies}	0.02, 0
	Price for public charging	p^{public}	EUR/kWh	0.50	
	Max. grid connection capacity	$P^{GCP,max}$	MW	5	0.7, 1, 1.5, 2
	Feed-in remuneration PV (ref)		EUR/kWh	0.06	
BET	Number of vehicles	n_{EV}		30	20, 40, 50
	Efficiency of charging	$\eta^{EV,charge}$		0.926	
	Efficiency of discharging	$\eta^{EV,discharge}$		0.921	
	Capacity vehicle battery	$E^{EV,max}$	kWh	250/500	
	Minimum SOC at departure	$SOC^{EV,dep,min}$		1	
	Maximum charging/ discharging power	$P^{EV,max}$	kW	100	50, 200
PV-System	Peak power		kW	1,000	0, 2,000
	Azimuth angle		°	0	
	Tilt angle		°	35	

Table 3: Year dependent parameters.

year	p_t^{ref} (EUR/kWh)	p^{levies} (EUR/kWh)	p_{usage} (EUR/kWh)	p_{cap} (EUR/kWh)
2019	0.038	0.131	0.047	16.37
2020	0.030	0.135	0.052	18.36
2021	0.097	0.133	0.054	18.65
2022	0.245	0.495	0.056	19.20

3 Results

In order to better understand the results presented in the following, we first look at a single example day. Therefore, a sunny weekday in August from the base scenario in 2021 is chosen. Figure 5 is intended to explain the charging strategies and shows the important time series from the optimization results for the example day. The results for the reference simulation are shown on the left and those for the bidirectional optimization are shown on the right. The unidirectional optimization is excluded due to space constraints. In the upper diagram, the power of the different components is plotted as a stacked area diagram. The resulting power at the grid connection point $P_t^{GCP} = P_t^{GCP,in} + P_t^{GCP,out}$ is shown as black line. The center diagram illustrates for each time step how many vehicles are attendant and how many of them are charging or discharging. The used prizes contains the lower diagram. Levies and gridfees are not included in the prices.

With uncontrolled reference charging, the vehicles are charged immediately when they arrive at the depot. Even though some vehicles arrive and charge at midday, this leads to charging processes in the evening and at night where power of the PV-system is unavailable. The unused energy from the PV system is fed into the grid for the low feed-in tariff and more expensive energy is purchased from the grid in the evening hours. The situation is different with the bidirectional charging strategy. According to the optimization problem presented in Chapter 2.1, the objective of the optimization is to maximize the revenue. One way to achieve this is to shift the charging process to times when PV power is available, since this power is not priced in the optimization problem. This shifting is clearly visible in the diagram because the area of the BET charging matches the PV-generation. Energy can also be fed into the grid to maximize the revenue. Such a feed-in takes place on the example day from approx. 6 PM, when many vehicles are available and high energy prices are reached. Due to the oversized grid connection capacity of 5 MW, a large number of BETs uncharge at the same time, resulting in a high feed-in power of over 2 MW. Because of the power price integrated in Equation (8), the annual power peak of the reference of 1.3 MW is lowered in the optimization to 0.4 MW. The power price only affects the purchased power,

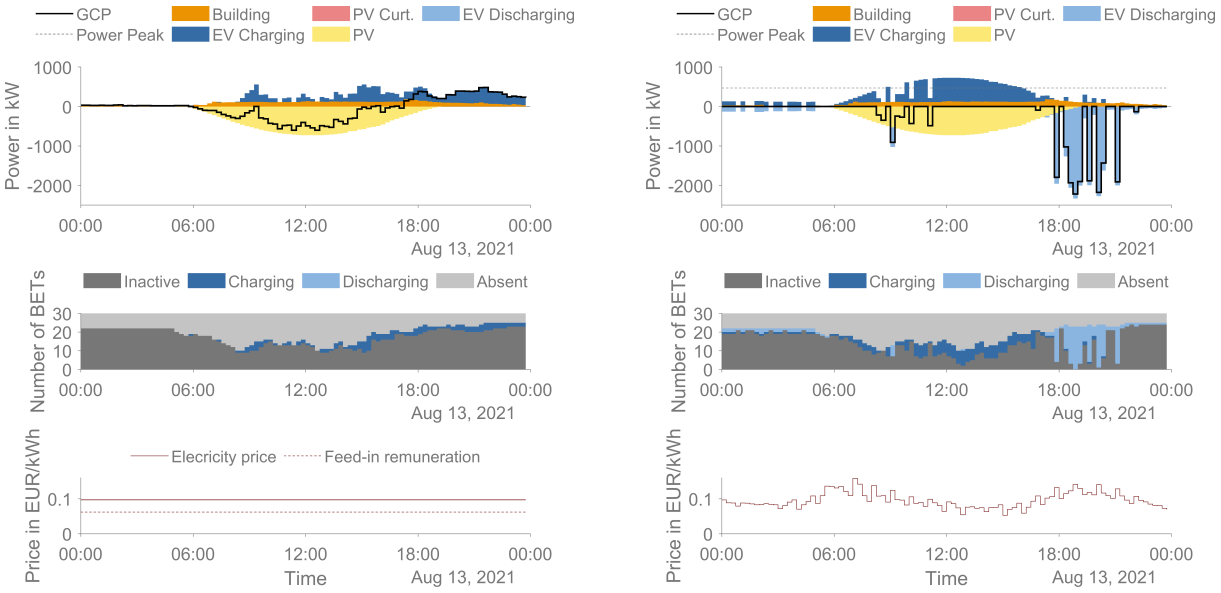

(a) Reference

(b) Bidirectional

Figure 5: Results for an example day for different charging strategies.

which allows the feed-in with a higher power. The diagram also clearly shows that outside the times with PV generation, the vehicles supply each other and also the building with energy.
The results of the base scenario are compared with those of the other examined years in Figure 6. Figure 6a shows the annual savings for the optimization with unidirectional (uni) and bidirectional (bidi) BETs. The savings are calculated from the difference between the costs in the reference simulation and the respective charging strategy and are normalized per vehicle. Before 2021, the savings are modest at less than 1,000 EUR/BET even with bidirectional vehicles. As energy prices rise from 2021 (cf. Fig. 3), savings also increase significantly. Thus, 2,200 EUR/BET can be achived in 2021 with the bidirectional and 1,000 EUR with the unidirectional charging strategy. In 2022 the savings skyrocket up to almost 12,000 EUR/BET. On the one hand, this can be explained by the fact that the reference costs in 2021 and 2022 rise due to the higher prices. On the other hand, the increasing price spreads and falling levies are responsible for the high savings, as this makes arbitrage trading significantly more attractive.
That can also be observed in Figure 6b, where the average discharged energy per BET and year is illustrated. It only represents the results from the bidirectional charging strategy, because only here discharging can occur. The diagram contains information on how much energy is fed back to the building (V2B), to other vehicles (V2V) or to the grid (V2G). Discharging into the grid takes place in order to generate revenues. V2G dominates the discharged energy in 2022 which explains the high revenues discussed above. Since the load of the building can not flexibly respond to prices and PV generation,

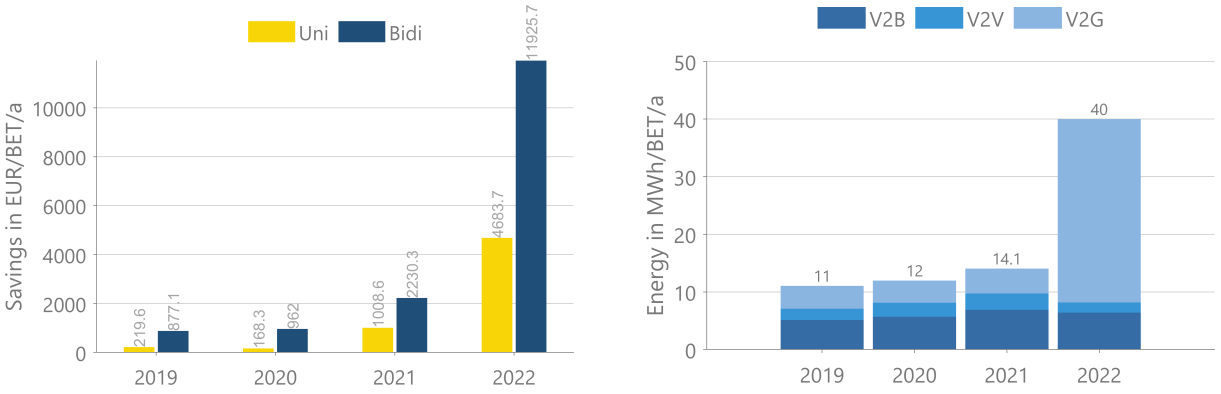

(a) Annual energy costs of the entire depot

(b) Discharged energy

Figure 6: Results of the analyzed years.

through discharging, the BET can supply the building with cheaper energy from the PV-system or the grid in time steps with high electricity prices. Furthermore, V2B can serve to reduce the annual power peak. The same applies for V2V, where vehicles are constrained by their driving behavior and thus cannot always charge at the convenient time steps. V2V is thus another way to achieve optimal charging costs. The share of V2B is relatively similar in all years and is slightly higher in 2021 and 2022 than in previous years. V2V takes the smallest share of the discharged energy in all years. In the reference scenario, the self-consumption rate is approx. 50% in all the examined years. The optimization increases this ratio to almost 65% unidirectional and 95% bidirectional.
In order to examine the influence of individual parameters on the results, the results of the sensitivity analysis for the bidirectional charging strategy are shown in Figure 7. The diagram shows on the x-axis the deviation of the varied parameter from the base scenario and on the y-axis the savings matching Figure 6a. The reduction of the grid connection capacity has the least impact on the savings. With the limitation of 700 kW, the connected load is still large enough and the savings decrease only minimally. A drastic reduction of $P^{GCP,max}$ would reduce the savings more significantly, but then the PV system has to be curtailed, and which is not considered reasonable for this paper. The savings decrease without a PV system but increase with a larger PV system. With higher charging and discharging power, savings can be increased. In the analysis, the charging power of 200 kW leads to increased savings above 2,700 EUR per BET. A larger number of vehicles reduces the savings per vehicle. The parameter with the strongest impact on the savings are the levies on the fed back energy. In the base scenario, the worst case is assumed that no exemption takes place. With full exemption, the annual savings per BET strongly increase to almost 8,000 EUR. However, these savings are only possible with a significant higher, discharged energy from the the BET to the grid.

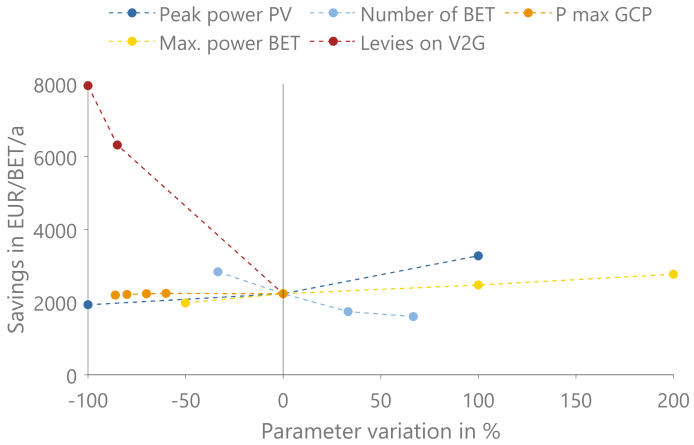

Figure 7: Results of the sensitivity analysis.

4 Conclusion and Outlook

This study clearly shows that the examined depot is very well-suited for the implementation of bidirectional charging strategies and that the operator of the depot can benefit monetarily from it. Due to the large PV system and the long durations of attendance of the BET, the depot under consideration offers excellent conditions for optimization. In the base scenario, the bidirectional charging strategy can save 2,200 EUR per vehicle and year compared to uncontrolled charging. In the optimization, the minimization of the costs is achieved by increase the self-consumption rate, reducing the annual peak load and performing arbitrage trading respectively charging at time steps with low energy prices. A self-consumption rate of 95% can be achieved and the peak load can be significantly reduced. Arbitrage trading is only worthwhile when price spreads are high. In addition, high levies prevent arbitrage trading if there is no exemption for electricity fed back into the grid. Such an exemption applies to stationary storage. The implementation of such an exemption is difficult especially for sites with PV. For such a side, it is impossible to exactly identify how much of the fed back energy comes from the grid and how much from the PV-system. A simplified approach for this problem is introduced in this paper.
This paper may form the basis for further research on the topic of bidirectional charging in depots for BETs. Since the results of this paper are only calculated for one example depot, it should be examined how well the results can be transferred to other depots. Therefore, data from further depots must be obtained and the calculations must be performed again with them. Especially the driving behavior of the BET from other depots could differ. It should also be analyzed if further use cases, such as providing frequency control, can be integrated into the optimization. In the present study, the investment costs of the PV system, the charging infrastructure and the grid connection capacity were not taken into account,

as only the energy costs were optimized. However, investment costs are also important for the implementation. The forwarder needs to know whether the lower charging costs through bidirectional charging compensate the investment costs for the bidirectional charging infrastructure. Otherwise, forwarders will not invest in the technology. Future studies should therefore consider these costs by using a Total Costs of Ownership (TCO) analysis.

Acknowledgments

This research was conducted as part of the activities of the FfE in the project NEFTON, funded by the Federal Ministry of Economics and Climate Action (BMWK) (funding code: 01MV21004E).

References

[1] J. Høj, L. Juhl, and S. Lindegaard, "V2G—An Economic Gamechanger in E-Mobility?" *WEVJ*, vol. 9, no. 3, p. 35, Aug. 2018. [Online]. Available: http://www.mdpi.com/2032-6653/9/3/35

[2] T. Kern and S. Kigle, "Modeling and evaluating bidirectionally chargeable electric vehicles in the future European energy system," *Energy Reports*, vol. 8, pp. 694–708, Dec. 2022. [Online]. Available: https://linkinghub.elsevier.com/retrieve/pii/S2352484722022120

[3] "Nissan approves first bi-directional charger for use with Nissan LEAF in the U.S." Sep. 2022. [Online]. Available: https://usa.nissannews.com/en-US/releases/nissan-approves-first-bi-directional-charger-for-use-with-nissan-leaf-in-the-us

[4] "CO2 emissions from heavy-duty vehicles Preliminary CO2 baseline (Q3-Q4 2019) estimate," Mar. 2022. [Online]. Available: https://www.acea.auto/files/ACEA_preliminary_CO2_baseline_heavy-duty_vehicles.pdf

[5] C. Cunanan, M.-K. Tran, Y. Lee, S. Kwok, V. Leung, and M. Fowler, "A Review of Heavy-Duty Vehicle Powertrain Technologies: Diesel Engine Vehicles, Battery Electric Vehicles, and Hydrogen Fuel Cell Electric Vehicles," *Clean Technol.*, vol. 3, no. 2, pp. 474–489, Jun. 2021. [Online]. Available: https://www.mdpi.com/2571-8797/3/2/28

[6] B. Nykvist and O. Olsson, "The feasibility of heavy battery electric trucks," *Joule*, vol. 5, no. 4, pp. 901–913, Apr. 2021. [Online]. Available: https://linkinghub.elsevier.com/retrieve/pii/S2542435121001306

[7] S. Link and P. Plötz, "Technical Feasibility of Heavy-Duty Battery-Electric Trucks for Urban and Regional Delivery in Germany—A Real-World Case Study," *WEVJ*, vol. 13, no. 9, p. 161, Aug. 2022. [Online]. Available: https://www.mdpi.com/2032-6653/13/9/161

[8] H. Liimatainen, O. van Vliet, and D. Aplyn, "The potential of electric trucks – An international commodity-level analysis," *Applied Energy*, vol. 236, pp. 804–814, Feb. 2019. [Online]. Available: https://linkinghub.elsevier.com/retrieve/pii/S0306261918318361

[9] M. Zähringer, S. Wolff, J. Schneider, G. Balke, and M. Lienkamp, "Time vs. Capacity—The Potential of Optimal Charging Stop Strategies for Battery Electric Trucks," *Energies*, vol. 15, no. 19, p. 7137, Sep. 2022. [Online]. Available: https://www.mdpi.com/1996-1073/15/19/7137

[10] R. Razi, K. Hajar, A. Hably, M. Mehrasa, S. Bacha, and A. Labonne, "Assessment of predictive smart charging for electric trucks: a case study in fast private charging stations," in *2022 IEEE International Conference on Electrical Sciences and Technologies in Maghreb (CISTEM)*. Tunis, Tunisia: IEEE, Oct. 2022, pp. 1–6. [Online]. Available: https://ieeexplore.ieee.org/document/10043874/

[11] S. Englberger, K. Abo Gamra, B. Tepe, M. Schreiber, A. Jossen, and H. Hesse, "Electric vehicle multi-use: Optimizing multiple value streams using mobile storage systems in a vehicle-to-grid context," *Applied Energy*, vol. 304, p. 117862, Dec. 2021. [Online]. Available: https://linkinghub.elsevier.com/retrieve/pii/S0306261921011843

[12] C. Roselli and M. Sasso, "Integration between electric vehicle charging and PV system to increase self-consumption of an office application," *Energy Conversion and Management*, vol. 130, pp. 130–140, Dec. 2016. [Online]. Available: https://linkinghub.elsevier.com/retrieve/pii/S0196890416309463

[13] T. Kern and B. Bukhari, "Peak shaving – a cost-benefit analysis for different industries," in *12. Internationale Energiewirtschaftstagung an der TU Wien*. Wien: TU Wien, 2021.

[14] F. Biedenbach and Z. Valerie, “Opportunity or Risk? Model-Based Optimization of Electric Vehicle Charging Costs for Different Types of Variable Tariffs and Regulatory Scenarios from a Consumer Perspective,” Porto (Portugal), Jun. 2022.

[15] T. Kern, P. Dossow, and S. von Roon, “Integrating Bidirectionally Chargeable Electric Vehicles into the Electricity Markets,” *Energies*, vol. 13, no. 21, p. 5812, Nov. 2020. [Online]. Available: https://www.mdpi.com/1996-1073/13/21/5812

[16] B. Battke and T. S. Schmidt, “Cost-efficient demand-pull policies for multi-purpose technologies – The case of stationary electricity storage,” *Applied Energy*, vol. 155, pp. 334–348, Oct. 2015. [Online]. Available: https://linkinghub.elsevier.com/retrieve/pii/S0306261915007680

[17] D. Parra and M. K. Patel, “The nature of combining energy storage applications for residential battery technology,” *Applied Energy*, vol. 239, pp. 1343–1355, Apr. 2019. [Online]. Available: https://linkinghub.elsevier.com/retrieve/pii/S0306261919302399

[18] T. Kern, P. Dossow, and E. Morlock, “Revenue opportunities by integrating combined vehicle-to-home and vehicle-to-grid applications in smart homes,” *Applied Energy*, vol. 307, p. 118187, Feb. 2022. [Online]. Available: https://linkinghub.elsevier.com/retrieve/pii/S0306261921014586

[19] M. Naumann, F. B. Spingler, and A. Jossen, “Analysis and modeling of cycle aging of a commercial LiFePO4/graphite cell,” *Journal of Power Sources*, vol. 451, p. 227666, Mar. 2020.

[20] Veronika Henze. Lithium-ion battery pack prices rise for first time to an average of $151/kwh. [Online]. Available: https://about.bnef.com/blog/lithium-ion-battery-pack-prices-rise-for-first-time-to-an-average-of-151-kwh/

[21] L. Yao, S. Xu, A. Tang, F. Zhou, J. Hou, Y. Xiao, and Z. Fu, “A review of lithium-ion battery state of health estimation and prediction methods,” *World Electric Vehicle Journal*, vol. 12, no. 3, p. 113, Aug. 2021.

[22] G. Balke and L. Adenaw, “Dataset of Trucks’ Anonymized Recorded Driving and Operation,” Feb. 2023, version Number: 1.0 Type: dataset. [Online]. Available: https://zenodo.org/record/7599687

[23] S. Sripad and V. Viswanathan, “Performance metrics required of next-generation batteries to make a practical electric semi truck,” *ACS Energy Letters*, vol. 2, pp. 1669–1673, 06 2017.

[24] M. Schroedter-Homscheidt, C. Hoyer-Klick, N. Killius, M. Lefèvre, L. Wald, E. Wey, and L. Saboret, “User’s guide to the cams radiation service - status december 2017,” 12 2017.

[25] EPEX-Spot SE, “Market data of epex-spot se,” 2023. [Online]. Available: https://www.epexspot.com

[26] BDEW, “Bdew electricity price analysis beginning of 2023,” 2023. [Online]. Available: https://www.bdew.de/service/daten-und-grafiken/bdew-strompreisanalyse/

[27] Netze BW GmbH, “Prices for the use of the electricity distribution grid of netze bw gmbh,” 2022. [Online]. Available: https://www.netze-bw.de/

Presenter Biography

Florian Biedenbach, M. Sc. received his master’s degree in renewable energy systems from the Technical University of Berlin in 2019. Since then, he has been a research associate at FfE in Munich (Germany), where he is working on the topic of electromobility. In the research project NEFTON, he is responsible for the simulation of charging scenarios. In the research project Trade-EVs II, he is project manager. In his dissertation, he will deal with the multi-use optimization of commercial battery electric fleets.